Interleukin-27 potentiates CD8+ T-cell-mediated anti-tumor immunity in chronic lymphocytic leukemia

Giulia Pagano,[1,2*] Iria Fernandez Botana,[1,2*] Marina Wierz,[1] Philipp M. Roessner,[3] Nikolaos Ioannou,[4] Xiangda Zhou,[5] Gheed Al-Hity,[4] Coralie Borne,[1] Ernesto Gargiulo,[1] Susanne Gonder,[1,2] Bin Qu,[5] Basile Stamatopoulos,[6] Alan G. Ramsay,[4] Martina Seiffert,[3] Anne Largeot,[1] Etienne Moussay[1#] and Jerome Paggetti[1#]

[1]Tumor Stroma Interactions, Department of Cancer Research, Luxembourg Institute of Health, Luxembourg, Luxembourg; [2]Faculty of Science, Technology and Medicine, University of Luxembourg, Esch-sur-Alzette, Luxembourg; [3]Molecular Genetics, German Cancer Research Center (DKFZ), Heidelberg, Germany; [4]School of Cancer and Pharmaceutical Sciences, Faculty of Life Sciences & Medicine, King's College London, London, UK; [5]Biophysics, Center for Integrative Physiology and Molecular Medicine, School of Medicine, Saarland University, Homburg, Germany and [6]Clinical Cellular Therapy Research Laboratory, Jules Bordet Institute, Brussels, Belgium

GP and IFB contributed equally as first authors.
#EM and JP contributed equally as senior authors.

Correspondence: J. Paggetti
jerome.paggetti@lih.lu

Received: November 22, 2022.
Accepted: June 15, 2023.
Early view: June 22, 2023.

https://doi.org/10.3324/haematol.2022.282474

Supplementary Information – Pagano, Fernandez-Botana, *et al*.

Interleukin-27 potentiates CD8$^+$ T cell-mediated anti-tumor immunity in Chronic Lymphocytic Leukemia

Materials and Methods

Animal experiments

Leukemic cells derived from *Eμ-TCL1* mice were adoptively transferred (AT) by i.p. or i.v. transplantation (1-2x10^7/100µl DMEM) into C57BL/6 wild type (WT), *Ebi3*$^{-/-}$ (Jax #008691), and *Rag2*$^{-/-}$ mice. All murine lines used were of C57BL/6 background. In specific experiments, CLL cells were injected after isolation from the spleen using the MojoSort™ Mouse Pan B Cell Isolation Kit (Biolegend) according to the manufacturer's instructions. Unless stated otherwise, all AT experiments were performed on sex and age-matched mice ranging from six to ten weeks of age. When applicable, CD3$^+$ T-cells were isolated from WT and *Ebi3*$^{-/-}$ splenocytes using the MojoSort™ Mouse CD3 T-cell Isolation Kit (Biolegend) according to the manufacturer's instructions, and co-injected with the *Eμ-TCL1* splenocytes. CLL progression in leukemic mice was monitored weekly by assessment of the percentage of CD5$^+$ CD19$^+$ cells in the PB. The blood cell count was determined using the MS4e Vet haematology analyser (Melet-Schloesing, France).

Mice were euthanized by cervical dislocation before reaching the established humane end-point, and the leukemic spleens were dissected and processed as previously described.

In vivo treatment with IL-27 neutralizing antibody or isotype IgG control (BioXcell, NH) was performed *i.p.* in *Eμ-TCL1*-AT mice. Antibody administration started two days prior to CLL AT and was repeated twice a week throughout the course of the experiment. For the first two injections, 500µg of anti-IL-27 neutralizing antibody were administered per mouse in 200µl of buffer (Day -2 and day 0). The following injections comprised 250µg of anti-IL-27 antibody in 100µl buffer. Blood serum was obtained weekly during routine blood checks by centrifuging the coagulated PB (2000g, 4°C, 20').

Flow cytometry

Cell sorting

$CD3^+$ T-cells were isolated from *FoxP3*$^{YFP/Cre}$ (Jax #016959, C57BL/6 background) and *FoxP3*$^{YFP/Cre}$ *Ebi3*$^{-/-}$ mice using MojoSort™ Mouse CD3 T-cell Isolation Kit (Biolegend), and activated with plate-bound anti-CD3 (2µg/ml), anti-CD28 (2µg/ml) and IL-2 (10 ng/mL) for 72 hours. Cells were harvested after three days, stained for surface markers and FACS-sorted using a FACSAria sorter III (BD Biosciences) in three fractions: $CD8^+$ T-cells, $CD4^+$ conventional T-cells and $FOXP3^+$ regulatory T-cells (Treg, YFP^+). The samples were immediately spun down (500g, 10'), resuspended in 500 µl of Nucleozol (Takara Bio) and frozen at -80°C.

Cell clustering

Clustering analysis of live lymphocytes was performed with Cytosplore software. Briefly, samples were randomly down-sampled and subjected to Hierarchical Stochastic Neighbor Embedding (HSNE) to generate clusters based on phenotypic similarities. Clusters were generated using the Gaussian mean shift algorithm using the density estimate as input.

T-cell-mediated cytotoxicity assay on murine CLL

Assessment of the cytotoxicity of IL-27-treated T-cells on murine CLL cells was performed as previously described [1]. Briefly, $CD3^+$ T-cells were isolated from C57BL/6 mice, cultured in RPMI1640 medium supplemented with 10% FBS, 1% P/S, and stimulated with coated anti-CD3 (1µg/ml) and soluble anti-CD28 (1µg/ml) for 48h at 37°C. Treatment with IL-27 was performed daily (25ng/ml). CLL cells ($CD5^+CD19^+$) isolated from *Eµ-TCL1* mice were stained with CellTrace CFSE (200nM, Thermo Fisher) and pulsed with 2µg/ml of super antigen (sAg; SEA and SEB; Sigma-Aldrich) for 30' at 37°C. The generated target CLL cells ($2.5x10^4$) were then loaded with sAg were added to the pre-treated $CD3^+$ T cells at a 1:20 (target: effector). Cell mixtures were centrifuged, and incubated for 4h at 37°C. Cells were stained with TO-PRO-3 viability dye (Thermo Fisher) according to the manufacturer's instructions and T-cell-mediated cytotoxicity against CLL target cells was determined by flow cytometry. Cytotoxicity was

calculated as: % target cell death = (% CFSE+ TO-PRO-3+ target cells incubated with effector T-cells - % of $CFSE^+$ $TO\text{-}PRO\text{-}3^+$ target cells incubated alone) × 100/(100 - % of $CFSE^+$ $TO\text{-}PRO\text{-}3^+$ target cells incubated alone).

T-cell-mediated cytotoxicity assay on patient-derived CLL samples

CLL patient-derived peripheral blood mononuclear cells (PBMCs) were divided into either "target cells" or cells for further processing. The latter were depleted from $CD19^+$ cells using a positive selection kit, enriched for $CD3^+$ T cells, and plated with or without IL-27 (100 ng/mL) antibody in 48-well plates previously coated with 1 µg/mL anti-CD3 antibody for 48 h at 37°C.

Prior to the cytotoxicity assay, the target cell fraction CLL cells were stained with CellTrace CFDA (200 nM) (Thermo Fisher) and pulsed with 1 µg/mL of sAgs (SEA and SEB) for 30 min at 37°C. Target cells ($2.5x10^4$) loaded with sAg were then added to the pre-treated effector T cells at a 1:20 (target:effector) ratio. Cell mixtures were centrifuged, and the cell pellets incubated for 4 h at 37°C. Target cells from each patient were centrifuged and incubated alone as a control for spontaneous/drug-induced cell death. Finally, cells were stained with TO-PRO-3 viability dye (Thermo Fisher) according to the manufacturer's instructions and T cell-mediated cytotoxicity against target cells was determined by flow cytometry. Cytotoxicity was calculated as: % target cell death = (% CFDA+ TO-PRO-3+ target cells incubated with effector T cells - % of CFSE+ TO-PRO-3+ target cells incubated alone) × 100 / (100 - % of CFDA+ TO-PRO-3+ target cells incubated alone).

Three-dimensional killing assay on human samples

The real-time killing assay was performed as previously described [2]. In summary, Human CD3/CD28 activator beads (ThermoFisher Scientific) were used to stimulate PBMCs (0.7:1 ratio Beads/PBMCs) with or without IL-27 (100 ng/ml) for 6 days at 37 °C with 5% CO2. On day 4, half of the media was replaced by fresh media. For the 3D killing assay, NALM6-pCasper cells [3] were pulsed with SEA and SEB (1µg/ml) at 37 °C with 5% CO2 for 30 min. The pulsed NALM6-pCapser cells were then embedded

into 2 mg/mL Type I bovine collagen (Advanced Biomatrix) and centrifuged down to the bottom as described before [2]. After gel solidification, PBMCs were placed on top of the collagen matrix at a 20:1 effector: target ratio. Live cell imaging was carried out using a high-content imaging system (ImageXpress, Molecular Devices) at 37 °C with 5% CO2 for 30 hours. Images were analyzed with ImageJ.

RNA sequencing

Previously sorted cells were thawed and RNA was isolated using the Nucleosol RNA isolation kit (Macherey-Nagel) prior to bulk-RNAseq. Librairies were prepared with the QuantSeq 3' mRNA-Seq Library Prep Kit FWD for Illumina (Lexogen), according to manufacturer's instructions, with the addition of UMI. Barcoded samples were pooled, diluted, loaded onto a NextSeq 500/500 Mid Output flowcell (130M reads, Illumina) and single-end sequencing was performed on a NextSeq 550 (Illumina).

RNA sequencing analysis

After initial QCs using FastQC and FastQ Screen tools made available by the Babraham Bioinformatics group (https://www.bioinformatics.babraham.ac.uk/projects), fastq files were processed using a local Snakemake workflow including the following main steps. First, raw reads were trimmed from their UMI index, poly A and adapter sequences using a combination of dedicated scripts and cutadapt (v2.10). Next, filtered reads were submitted for mapping (STAR v2.5.3a) on the Mouse Reference genome (GRCm38). Collapsing of reads originating from the same fragment was achieved with umi_tools (v 1.0.0) and counting was performed with featureCounts (subread v2.0.0).

Counts were filtered and transformed with EdgeR for clustering and principal component analysis (PCA). Differential expression of genes (DEG) across $CD8^+$ T-cells, Tconv and Treg cell samples was assessed using the NOISeq R/Bioconductor packages, and a FDR of 0.05 and a log2 fold change cut-off of 1 were imposed.

Immunofluorescence

$1x10^6$ cells were transferred in a U-bottom 96 well plate. PFA was added at a final concentration of 3.7%. After 15min of incubation at RT, the cells were washed with PBS, and centrifuged at 500g for 5min. Cells were permeabilized with 0.5% Triton x-100 in PBS for 15min at RT. After 2 washes with PBS, cells were blocked with the blocking buffer (1% BSA, 0.5% Triton X-100 in PBS) for 1h at RT. After washes, cells were incubated o.n. with the primary antibodies diluted in blocking buffer (anti-Profilin1, Cell Signalling, #3237, AB_2236990 and anti-CD8, Biolegend, #100705, AB_312744).

After 3 washes of 10min in permeabilization buffer, the cells were incubated 1h at RT with the secondary antibodies. The cells were then washed 3 times for 10min in permeabilization buffer. DAPI and actistain were added in the second wash. The cells were resuspended in Ibidi mounting medium and let to settle for 24h at 4°C in an Ibidi chamber (µ-Slide angiogenesis). Images were acquired on a confocal laser scanning microscope (LSM810; Zeiss) and analyzed with ImageJ.

Cytokine measurements

The levels of IL-27 in patient blood serum, as well as in murine blood serum and spleen plasma were quantified by ELISA using the LEGEND MAX™ Human IL-27 ELISA Kit (Biolegend) and LEGEND MAX™ Mouse IL-27 Heterodimer ELISA Kit (Biolegend), respectively, according to the manufacturer's instructions. Equal volumes of serum or spleen plasma were loaded across conditions.

Real-time PCR

Cell populations sorting

Leukemic C57BL/6 wild type (WT), previously AT with *Eµ-TCL1*-derived splenocytes, were euthanized before reaching the humane end-point and the leukemic spleens were dissected and processed. Cell suspensions were then stained for surface markers and sorted into five fractions using a Symphony sorter (BD Biosciences): CLL cells ($CD19^+$), $CD8^+$ T-cells ($CD19^-$ $NK1.1^-$ $CD3^+CD8^+CD4^-$) $CD4^+$ T-cells ($CD19^-$

NK1.1$^-$CD3$^+$CD8$^-$CD4$^+$), dendritic cells (CD19$^-$NK1.1$^-$Ly-6G$^-$CD11c$^+$CD11b$^+$) and monocytes/macrophages (CD19$^-$NK1.1$^-$Ly-6G$^-$CD11c$^-$CD11b$^+$). The sorted populations were immediately spun down (500g, 10min), resuspended in Nucleozol and frozen at -80°C.

RNA isolation

RNA from whole splenocytes or sorted cell types was isolated using the NucleoSpin RNA Set for NucleoZOL Mini kit according to manufacturer's instructions (Macherey-Nagel) and quantified with Nanodrop (Thermo Scientific).

Gene expression in cells

Reverse transcription of mRNA was performed in a SimpliAmp™ Thermal Cycler (ThermoFisher) using FastGene® Scriptase II cDNA 5x ReadyMix (Nippon genetics). Real-time PCR was performed in the QuantStudio™ 5 Real-Time PCR System (ThermoFisher) using the Takyon Low Rox SYBR 2XMaster Mix blue dTTP (Eurogentec). The primer sequences were as follows: *Ebi3* F: 5'- CTTCTCGGTATCCCGTGGC -3' and R: 5'- ACCGAGCCTGTAAGTGGCAAT -3', *Il27p28* F: 5'- TGTCCACAGCTTTGCTGAAT-3' and R: 5'- CCGAAGTGTGGTAGCGAGG-3', *18S* F: 5'- CCGCCGCCATGTCTCTAGT-3' and R: 5'- CTTTCCTCAACACCACATGAGC-3'

Analysis of publicly available data sets

For the analysis of Ebi3 gene expression, we collected raw or processed data from the GSE18026, GSE35179, GSE66858, GSE8835, and GSE8836 datasets (GEO database, NCBI). We used gene expression data from several CD8$^+$ T-cell populations for comparison [4]. Expression of differentially expressed genes from clusters 1-10 was gathered for PCA and clustering analysis.

1. Ioannou, N., et al., *Triggering interferon signaling in T cells with avadomide sensitizes CLL to anti-PD-L1/PD-1 immunotherapy.* Blood, 2021. **137**(2): p. 216-231.
2. Zhao, R., et al., *Targeting the Microtubule-Network Rescues CTL Killing Efficiency in Dense 3D Matrices.* Front Immunol, 2021. **12**: p. 729820.
3. Knorck, A., et al., *Cytotoxic Efficiency of Human CD8(+) T Cell Memory Subtypes.* Front Immunol, 2022. **13**: p. 838484.
4. Beltra, J.C., et al., *Developmental Relationships of Four Exhausted CD8(+) T Cell Subsets Reveals Underlying Transcriptional and Epigenetic Landscape Control Mechanisms.* Immunity, 2020. **52**(5): p. 825-841 e8.

Figure legends

Figure S1: *Ebi3*$^{-/-}$ transgenic mice do not produce IL-27 and display a TME with immunosuppressive features.

(A) Relative mRNA levels of the IL-27 subunits, p28 and Ebi3, in splenocytes of WT and *Ebi3* $^{-/-}$ mice. **(B)** Number of circulating neoplastic CD5^{+} CD19^{+} cells (n=18 for Ctrl and n=19 for *Ebi3*$^{-/-}$, two-way ANOVA), same mice as Fig 1A. **(C)** Experimental scheme and relative mRNA levels of the IL-27 subunits (*Ebi3* and *Il27p28*) in murine CLL cells, CD8^{+} T cells, CD4^{+} T cells, dendritic cells, monocytes/macrophages (relative to the housekeeping gene 18S) sorted from the spleen of leukemic mice (AT with TCL1 splenocytes; n=4. **(D-I)** The data shown corresponds to one experimental cohort of AT mice (n=9 for Ctrl and n=10 for *Ebi3*$^{-/-}$) as for Fig.1B-F **(D)** Cell numbers of CD8^{+} T cells, CD4^{+} Tconv, and Tregs in the spleen are compared between the two groups. **(E)** HSNE plots (Cytosplore) and heatmap depicting the expression of CD44, Ki-67, PD1, IFN-γ, TIGIT and CD62L on Ctrl and *Ebi3*$^{-/-}$ CD8^{+} T cells. **(F)** Percentages of CD8^{+} T-cell cluster distribution in Ctrl and *Ebi3*$^{-/-}$ CD8^{+} T cells**. (G)** Frequency of CD4^{+} Tconv with a naive (CD62L^{+} CD44^{-}), effector (CD62L^{-} CD44^{+}) or memory (CD62L^{+} CD44^{+}) phenotype among Ctrl and *Ebi3*$^{-/-}$ mice. **(H)** HSNE plots (Cytosplore) and heatmap depicting the expression of CD44, Foxp3, Ki-67, PD-1, IFN-γ, TIGIT and CD62L expression measured by FC on Ctrl and *Ebi3*$^{-/-}$ CD4^{+} T cells. **(I)** Percentages of cluster distribution on Ctrl and *Ebi3*$^{-/-}$ CD4^{+} T cells. Unpaired t test, * *P*< .05, ** *P*< .01, *** *P*< .001, **** *P*< .0001.

Figure S2: EBI3 depletion does not affect myeloid cell compartment and mildly affects T-cell distribution in a non-tumoral context.

(A-F) Healthy *Foxp3*$^{YFP/Cre}$ and *Foxp3*$^{YFP/Cre}$ *Ebi3*$^{-/-}$ mice (n=3 per group) were euthanized at 8 weeks of age and their splenocytes analyzed using FC. **(A)** Frequency of indicated cell populations among total live cells. T= T cells; NK= Natural killer cells; NKT= natural killer T cells; Myelo= myeloid cells. **(B)** Frequency of indicated cell populations out of CD11b^{+} cells. Neutro=neutrophils; DCs=dendritic cells; Mono=monocytes; Macro=macrophages. **(C)** Frequency of T-cell subpopulations among total T cells.

(D-F) $CD8^+$ and $CD4^+$ T cells were isolated from *Foxp3*$^{YFP/Cre}$ and *Foxp3*$^{YFP/Cre}$ *Ebi3*$^{-/-}$ splenocytes, stimulated *ex vivo* with PMA (80nM), ionomycin (1,3 mM) and brefeldin A (5µg/ml) and analyzed by FC. Frequency of indicated immune checkpoints and cytokines in **(D)** $CD8^+$ effector T cells, **(E)** $CD4^+$ Tconv cells and **(F)** Tregs after *ex vivo* stimulation. Unpaired t test, ** *P*< .01.

Figure S3: EBI3 depletion in transgenic Eµ-TCL1 mice promotes an immunosuppressive TME.

(A) Number of circulating leukemic cells in T and TE mice (n=17 in T mice and n=14 in TE mice. **(B-J)** Leukemic T and TE mice were euthanized and their splenocytes were processed and analyzed by FC (n=5 in T mice and n=6 in TE mice). **(B)** Percentage of CLL cells among splenocytes of T and TE mice. **(C)** Number of CLL cells in the spleen of T and TE mice. **(D)** Heatmap and HSNE plots depicting the expression of individual markers included in the clustering analysis of $CD8^+$ T cells derived from T and TE transgenic mice based on the expression of CD44, Ki-67, PD1, KLRG1, TIGIT, and CD62L measured by FC. (**E)** Percentages of $CD8^+$ T-cell clusters distribution on T and TE. **(F)** Percentage of $CD4^+$ T cells in the spleen of T and TE transgenic mice. **(G-H)** HSNE clustering analysis of T and TE $CD4^+$ T cells based on the expression of CD44, FOXP3, Ki-67, PD1, KLRG1 and CD62L measured by FC. Heatmap comprising the clusters and HSNE plots depicting the expression of individual markers. (**I)** Percentages of cluster distribution in $CD4^+$ T cells in T and TE mice. **(J)** CLL cells were isolated from T and TE mice (n=3 mice per group) and activated for 48h *in vitro*. CLL cells were stained and analyzed by FC. Unpaired t test, * *P*< .05, ** *P*< .01.

Figure S4: Specific T-cell-EBI3 depletion leads to a more immunosuppressive TME.

(A) Number of circulating T cells in recipient *Rag2*$^{-/-}$ mice injected with either Ctrl or *Ebi3*$^{-/-}$ $CD3^+$ T cells. **(B)** HSNE clustering analysis of Ctrl and *Ebi3*$^{-/-}$ $CD8^+$ T cells based on PD1, CD25, LAG3, CD127, TIGIT and CD44 expression measured by FC. Heatmap comprising the clusters generated by HSNE analysis and HSNE plots depicting the expression of individual markers. **(C)** Percentages of cells in clusters from $CD8^+$ T cells isolated from the spleen of recipient *Rag2*$^{-/-}$ mice. **(D)** HSNE clustering analysis of Ctrl and

Ebi3$^{-/-}$ CD4^{+} T cells based on ROR-γt, FOXP3, CD25, Ki-67, GATA3, CD103, T-bet, and GITR expression measured by FC. Heatmap comprising the clusters generated by HSNE analysis and HSNE plots depicting the expression of individual markers. **(E)** Percentages of cluster distribution in WT and *Ebi3*$^{-/-}$ CD4^{+} T cells. Unpaired t test, * $P < .05$.

Figure S5: CD8^{+} T cells, but not Tconv or Tregs, show major transcriptional changes in the absence of EBI3.

(A) Heatmap comparing the transcriptome of Ctrl and *Ebi3*$^{-/-}$ CD8^{+} T cells. **(B)** Heatmaps depicting the transcriptional changes associated with translation initiation (left) and rRNA processing (right) between Ctrl and *Ebi3*$^{-/-}$ CD8^{+} T cells. **(C)** Heatmap depicting the similarity of *Ebi3*$^{-/-}$ CD8^{+} T cells with subsets of exhausted T cells described in [4]. **(D)** Principal component analysis (PCA) of *Ebi3*$^{-/-}$ CD8^{+} T cells with the aforementioned subsets. **(E-F)** Volcano plot showing differentially expressed genes (DEG) in Ctrl and *Ebi3*$^{-/-}$ **(E)** Tregs and **(F)** Tconv.

Figure S6: *Ebi3* depletion in CD8^{+} T cells does not affect cytokine production after 3 days of activation.

(A) Frequency of cells expressing the selected markers in Ctrl vs *Ebi3*$^{-/-}$ CD8^{+} T cells after 3 days of activation. **(B-C)** HSNE clustering analysis of Ctrl and *Ebi3*$^{-/-}$ CD8^{+} T cells based on IL-2, Ki-i67, IFN-γ, CD44, CD39 and Granzyme B expression measured by FC at day 3 post activation. HSNE plots depicting the expression of individual markers. **(D)** Percentages of cluster distribution of Ctrl vs *Ebi3*$^{-/-}$ CD8^{+} T cells after 6 days of activation. **(E)** Cytotoxicity of *Ebi3*$^{-/-}$ CD8^{+} T cells in absence or presence of IL-27 against TCL1 splenocytes. **(F)** Experimental design of the 3D killing assay. Human PBMCs were isolated from four healthy donors and activated *in vitro* for 6 days in presence or absence of rhIL-27. At day 6, pulsed NALM6 cells transfected with the viability pCasper vector were added to the culture for 30h and live cell imaging was recorded. (scale bar, 50μm) Percentage of living target cells was calculated in the 3 conditions (activated PBMCs only, and in presence or absence of IL-27). **(G)** Bar chart showing the percentage of living target cells 10 hours after the start of the killing activity of CD8^{+} T cells. **(H)**

Individual plots representing the kinetic of cell killing for the four donors. Unpaired t test, ** *P*< .01, *** *P*< .001.

Figure S7: IL-27 does not affect human and murine CLL cells

(A) Relative gene expression of *EBI3* in different human cell subsets in CLL patients and healthy controls. **(B)** Relative gene expression of *Ebi3* in different murine cell subsets in Ctrl and *Eμ-TCL1* mice. **(C)** Viability **(D)** and phenotype of patient-derived CLL cells after 48h of treatment with increasing levels of IL-27. **(E)** Viability and **(F)** phenotype of *Eμ-TCL1*-derived splenocytes after 48h of treatment with increasing levels of IL-27. Unpaired T test, * P< .05, ** P< .01.

Figure S8: IL-27 neutralization partially recapitulates the less immunosuppressive microenvironment observed in the transgenic mouse model.

(A) Percentage of $CD8^+$ T among total T cells. **(B-C)** HSNE clustering analysis of splenic $CD8^+$ T cells from isotype- and α-IL-27-treated mice based on CD62L, TIGIT, KRLG1, PD1, Ki-67, and CD44 expression measured by FC. Heatmap comprising the clusters generated by HSNE analysis and HSNE plots depicting the expression of individual markers **(D)** Percentages of cluster distribution between $CD8^+$ T cells derived from the spleen of isotype- or α-IL-27-treated mice. **(E)** Percentage of $CD4^+$ T cells out of total T cells. **(F)** Percentage of Tconv and Tregs out of $CD4^+$ T cells. **(E)** Frequency of the indicated Treg populations. **(G)** HSNE clustering analysis and heatmap of splenic $CD4^+$ T cells from isotype- and α-IL-27-treated mice based on CD62L, TIGIT, KRLG1, PD1, Ki-67, and CD44 expression measured by FC. **(H)** Percentages of cluster distribution between splenic $CD4^+$ T cells from isotype- or α-IL-27-treated mice. Unpaired T test, * P< .05.

Supplemental Table 1: List of antibodies used in flow cytometry

Antigen	Fluorochrome	Clone	Specificity	Manufacturer	Product #	Other name	RRIDs
CD103	APC	2E7	Mouse	Biolegend	121414		AB_1227502
CD11b	PE-Cy7	M1/70	Mouse/Human	Biolegend	101215		AB_312798
CD11c	APC-V770	1B29	Mouse	Miltenyi	130-107-461		AB_2783921
CD134	APC	REA625	Mouse	Miltenyi	130-109-742	OX40	AB_2654942
CD152	PE	UC10-4B9	Mouse	Biolegend	106305	CTLA4	AB_313255
CD19	FITC	eBio1D3	Mouse	ThermoFisher	11-0193-86		AB_657665
CD19	PE-Cy7	eBio1D3	Mouse	ThermoFisher	25-0193-82		AB_657663
CD19	APC	6D5	Mouse	Biolegend	115512		AB_313647
CD19	Biotin	6D5	Mouse	Miltenyi	130-101-951		AB_2801732
CD25	BV421	PC61	Mouse	Biolegend	102043	IL-2Rα	AB_11203373
CD25	FITC	REA568	Mouse	Miltenyi	130-108-999		AB_2656653
CD25	BV421	PC61	Mouse	Biolegend	102043		AB_2562611
CD279	BV510	29F.1A12	Mouse	Biolegend	135241	PD-1	AB_2715761
CD3	PerCP	1B8	Mouse	Biolegend	100326		AB_893317
CD3	Biotin	1B3	Mouse	Miltenyi	130-109-835		AB_2751822
CD357	PerCP/Cy5.5	DTA-1	Mouse	Biolegend	126316	GITR	AB_2563384
CD39	PE-Cy7	Duha59	Mouse	Biolegend	143805		AB_2563393
CD4	APC-Fire 750	1B13	Mouse	Biolegend	100568		AB_2629699
CD4	APC-Cy7	RM4-5	Mouse	Biolegend	100526		AB_312727
CD44	FITC	IM7	Mouse	Biolegend	103022		AB_312957
CD44	AF700	IM7	Mouse	Biolegend	103026		AB_493713
CD44	PE	IM7	Mouse	Biolegend	103008		AB_312959
CD44	APC	IM7	Mouse/Human	Biolegend	103012		AB_312963
CD5	PE	53-7.3	Mouse	Biolegend	100608		AB_312737
CD5	APC	53-7.3	Mouse	Biolegend	100626		AB_2563929
CD62L	PE-Cy7	MEL-14	Mouse	Biolegend	104418		AB_313103
CD69	AF700	FN50	Human	Biolegend	310922		AB_493775
CD73	APC	TY/11.8	Mouse	Biolegend	127209		AB_11218786
CD8	BV650	1B21	Mouse	Biolegend	100742		AB_2563056
F4/80	BV421	BM8	Mouse	Biolegend	123137		AB_11203717
Foxp3	APC	REA788	Mouse	Miltenyi	130-111-601		AB_2651766
Foxp3	BV488	MF-14	Mouse	Biolegend	126406		AB_1089113
GATA3	BV421	16E10A23	Mouse/Human	Biolegend	653814		AB_2563221
Granzyme B	PE	QA16A02	Mouse/Human	Biolegend	372208		AB_2687032
HLA-A,B,C	PE-Cy7	W6/32	Human	Biolegend	311430		AB_2561617
IFNy	BV711	XMG1.2	Mouse	Biolegend	505836		AB_2650928
IL-10	BV421	JES3-9D7	Human	Biolegend	501421		AB_10896947

IL17A	PE	TC11-18H10	Mouse	Miltenyi	130-102-344		AB_2660786
IL2	PE-Cy7	JES6-5H4	Mouse	Biolegend	503832		AB_2561750
Ki-67	BV421	16A8	Mouse	Biolegend	652411		AB_2562663
Ki-67	APC	16A8	Mouse	Biolegend	652406		AB_2561930
Ki-67	BV421	16A8	Mouse	Biolegend	652411		AB_2562663
KLRG1	BV711	2F1/KLRG1	Mouse	Biolegend	138427	MAFA	AB_2629721
LAG-3	BV421	C9B7W	Mouse	Biolegend	125221	CD223	AB_2572080
LAG-3	APC	7H2C65	Human	Biolegend	369211	CD223	AB_2728372
Ly6c	PE	1G7.G10	Mouse	Miltenyi	130-102-391		AB_2857638
Ly6G	Biotin	REA526	Mouse	Miltenyi	130-107-911	Gr-1	AB_2727584
MHC-DR	APC	L243	Human	Biolegend	980406		AB_2650655
MHC-I	PE	28-8-6	Mouse	Biolegend	114607		AB_313598
MHC-II	BV650	M5/114.15.2	Mouse	Biolegend	107641	I-A/I-E	AB_2565975
NK1.1	Biotin	PK136	Mouse	Miltenyi	130-101-888	CD161	AB_2727573
PD-L1	APC	29E2A3	Human	Biolegend	329707	CD274	AB_940358
PD-L1	APC	29E2A3	Human	Biolegend	329707	CD274	AB_940358
RORg (t)	PE	B2D	Mouse	eBioscience	2054914		AB_10805392
Tbet	PE-Cy7	4B10	Mouse/Human	Biolegend	644823		AB_2561760
TGF-β	PerCP/Cy5.5	TW7-16B4	Mouse	Biolegend	141409		AB_2561591
TIGIT	PE	GIGD7	Mouse	eBiosciences	12-950182		AB_11042152
TNFa	APC	MP6-XT22	Mouse	Biolegend	506308		AB_315429
TOX	PE	TXRX10	Mouse	eBioscience	12-6502-82		AB_10855034

eBioscience™ Fixable Viability Dye eFluor® 506	ThermoFisher	65-0866-18	
Zombie Green™ Fixable Viability Kit	Biolegend	423111	
Zombie RED™ Fixable Viability Kit	Biolegend	423109	
Zombie UV™ Fixable Viability Kit	Biolegend	423108	
Zombie NIR™ Fixable Viability Kit	Biolegend	423106	

Figure S1

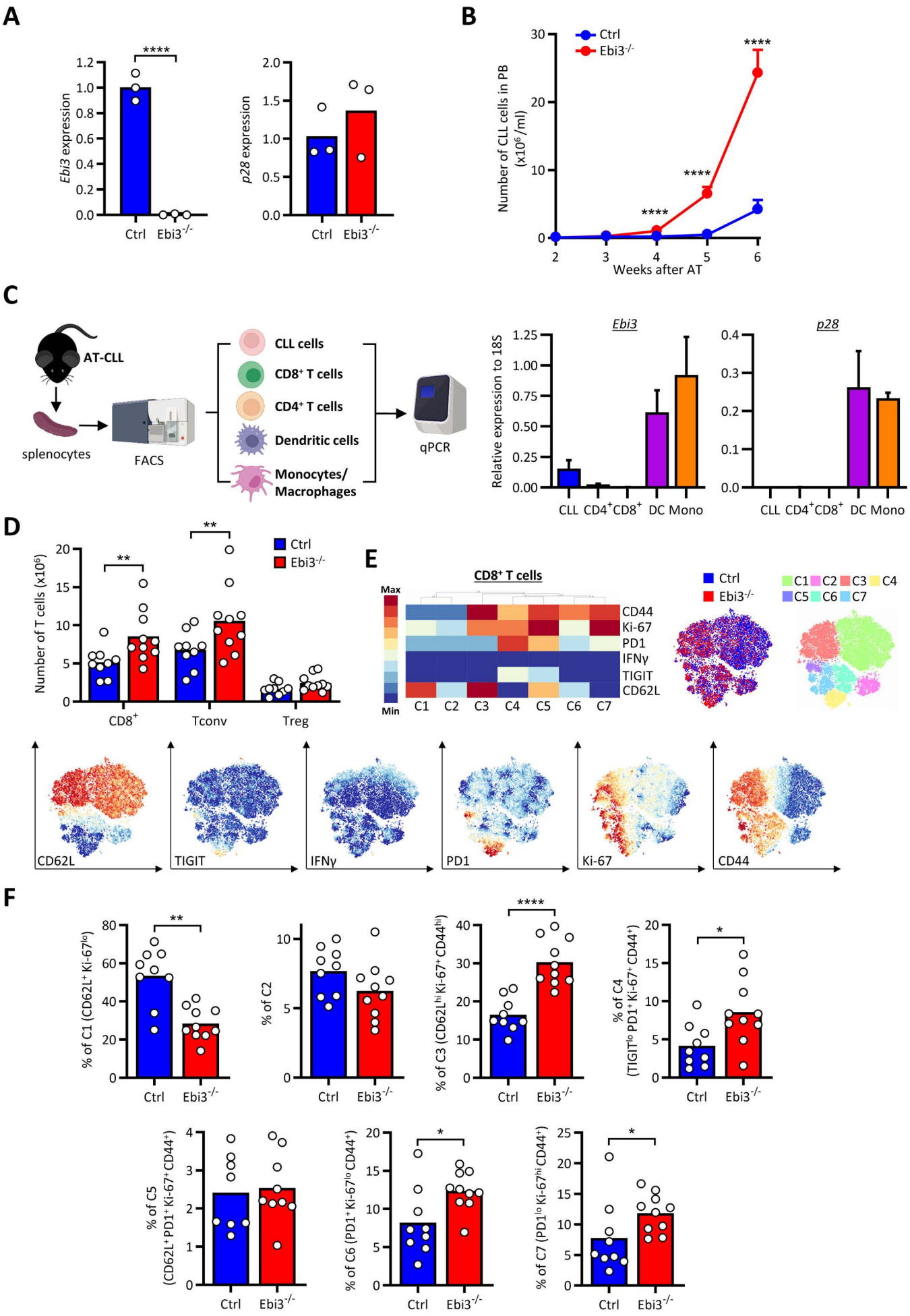
A
Ebi3 expression
p28 expression
Ctrl
Ebi3-/-
****
B
Number of CLL cells in PB (x10^6/ml)
Weeks after AT
Ctrl
Ebi3-/-
****
C
AT-CLL
splenocytes
FACS
CLL cells
CD8+ T cells
CD4+ T cells
Dendritic cells
Monocytes/ Macrophages
qPCR
Ebi3
p28
Relative expression to 18S
CLL CD4+CD8+ DC Mono
D
Number of T cells (x10^6)
CD8+
Tconv
Treg
E
CD8+ T cells
Max
Min
CD44
Ki-67
PD1
IFNγ
TIGIT
CD62L
C1 C2 C3 C4 C5 C6 C7
F
% of C1 (CD62L+ Ki-67lo)
% of C2
% of C3 (CD62Lhi Ki-67+ CD44hi)
% of C4 (TIGITlo PD1+ Ki-67+ CD44+)
% of C5 (CD62L+ PD1+ Ki-67+ CD44+)
% of C6 (PD1+ Ki-67lo CD44+)
% of C7 (PD1lo Ki-67hi CD44+)

Figure S1

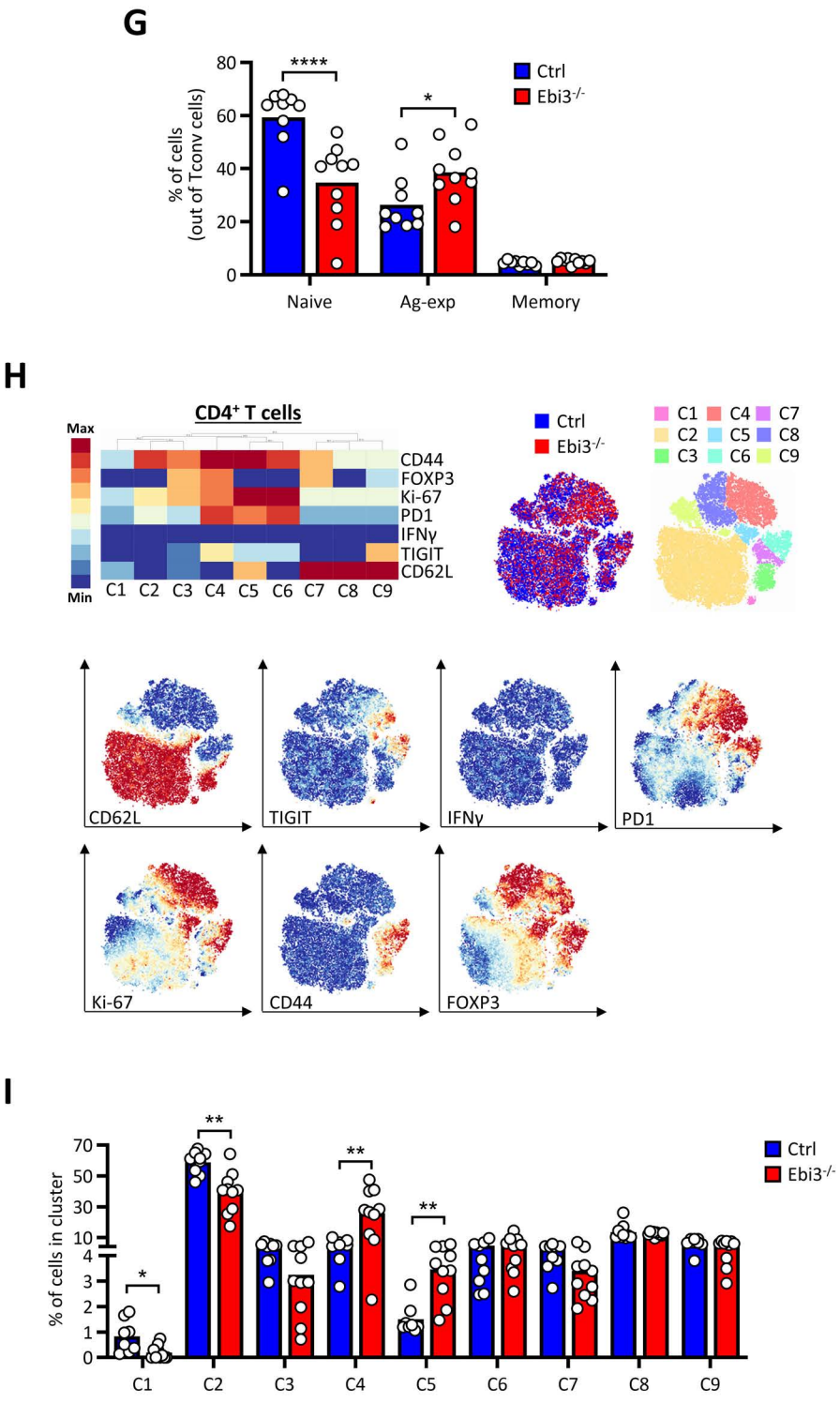
G
80
60
40
20
0
% of cells
(out of Tconv cells)
****
*
Ctrl
Ebi3-/-
Naive
Ag-exp
Memory
H
CD4+ T cells
Max
Min
CD44
FOXP3
Ki-67
PD1
IFNγ
TIGIT
CD62L
C1 C2 C3 C4 C5 C6 C7 C8 C9
Ctrl
Ebi3-/-
C1 C4 C7
C2 C5 C8
C3 C6 C9
CD62L
TIGIT
IFNγ
PD1
Ki-67
CD44
FOXP3
I
70
50
30
10
4
3
2
1
0
% of cells in cluster
*
**
**
**
Ctrl
Ebi3-/-
C1 C2 C3 C4 C5 C6 C7 C8 C9

Figure S2

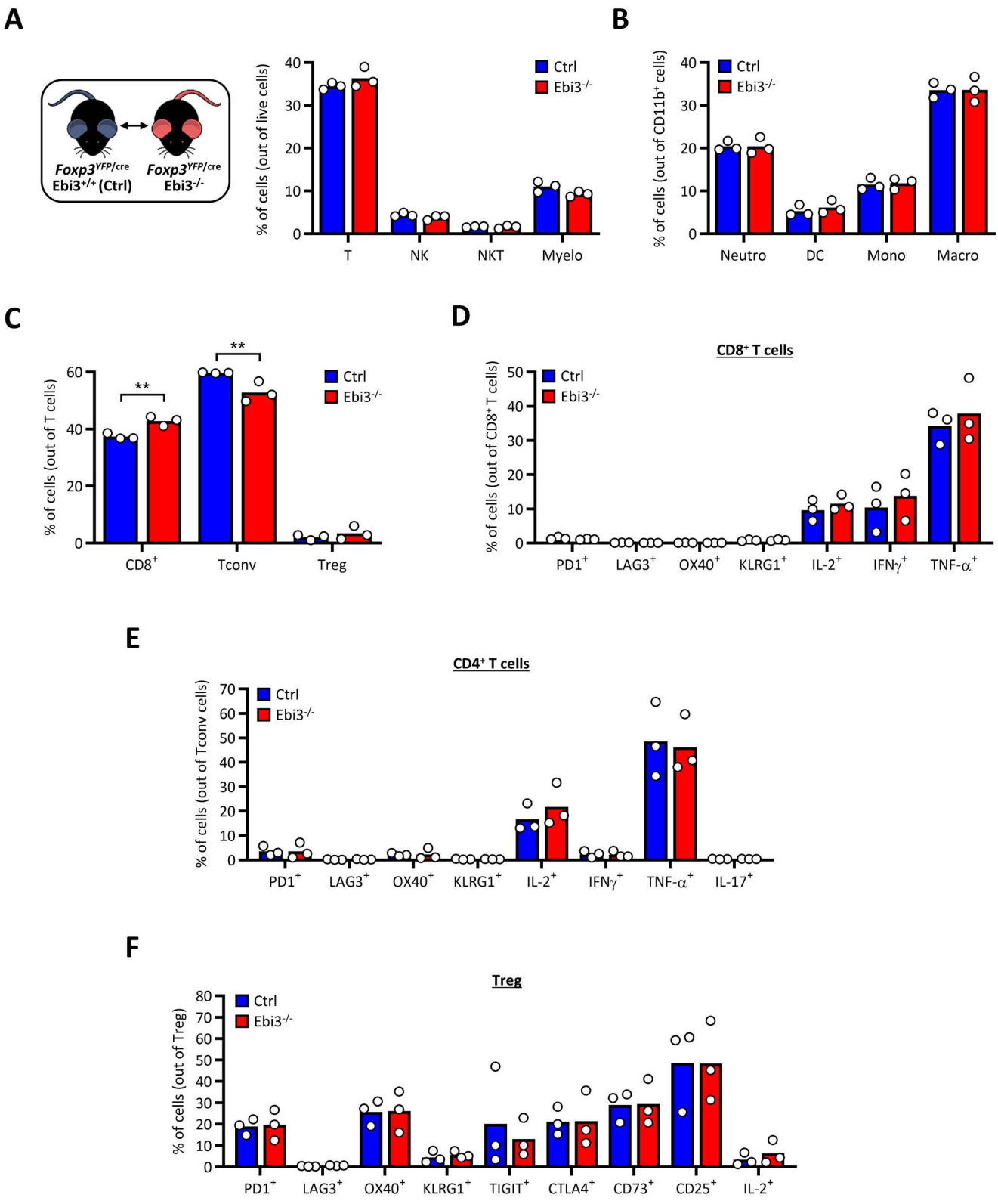
A
Foxp3YFP/cre Ebi3+/+ (Ctrl)
Foxp3YFP/cre Ebi3-/-
% of cells (out of live cells)
Ctrl
Ebi3-/-
T
NK
NKT
Myelo
B
% of cells (out of CD11b+ cells)
Neutro
DC
Mono
Macro
C
% of cells (out of T cells)
**
**
CD8+
Tconv
Treg
D
CD8+ T cells
% of cells (out of CD8+ T cells)
PD1+
LAG3+
OX40+
KLRG1+
IL-2+
IFNγ+
TNF-α+
E
CD4+ T cells
% of cells (out of Tconv cells)
PD1+
LAG3+
OX40+
KLRG1+
IL-2+
IFNγ+
TNF-α+
IL-17+
F
Treg
% of cells (out of Treg)
PD1+
LAG3+
OX40+
KLRG1+
TIGIT+
CTLA4+
CD73+
CD25+
IL-2+

Figure S3

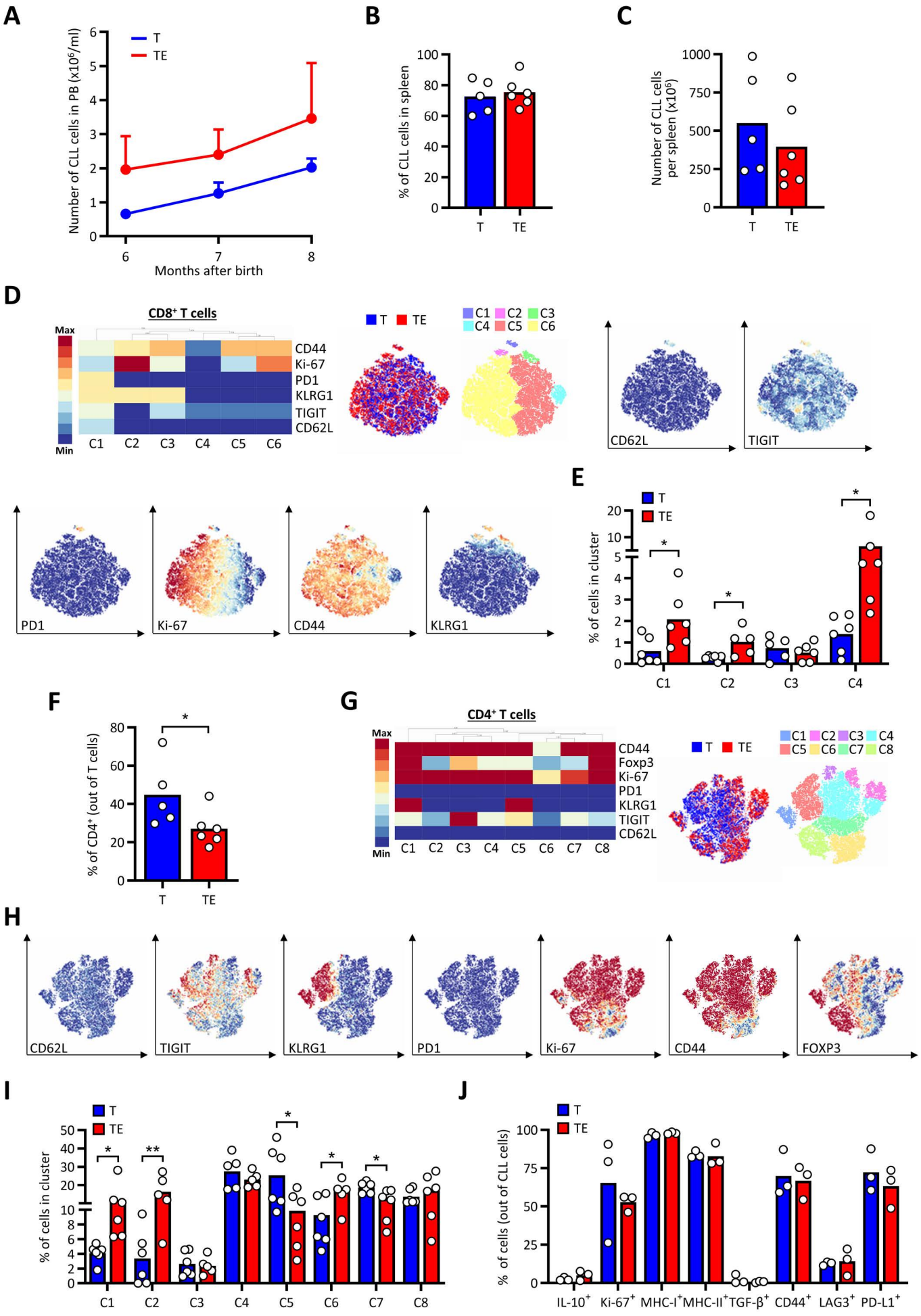
A
Number of CLL cells in PB (x10⁶/ml)
T
TE
Months after birth
B
% of CLL cells in spleen
C
Number of CLL cells per spleen (x10⁶)
D
CD8⁺ T cells
Max
Min
CD44
Ki-67
PD1
KLRG1
TIGIT
CD62L
C1 C2 C3 C4 C5 C6
E
% of cells in cluster
F
% of CD4⁺ (out of T cells)
G
CD4⁺ T cells
Foxp3
C7 C8
H
FOXP3
I
J
% of cells (out of CLL cells)
IL-10⁺ Ki-67⁺ MHC-I⁺ MHC-II⁺ TGF-β⁺ CD44⁺ LAG3⁺ PD-L1⁺

Figure S4

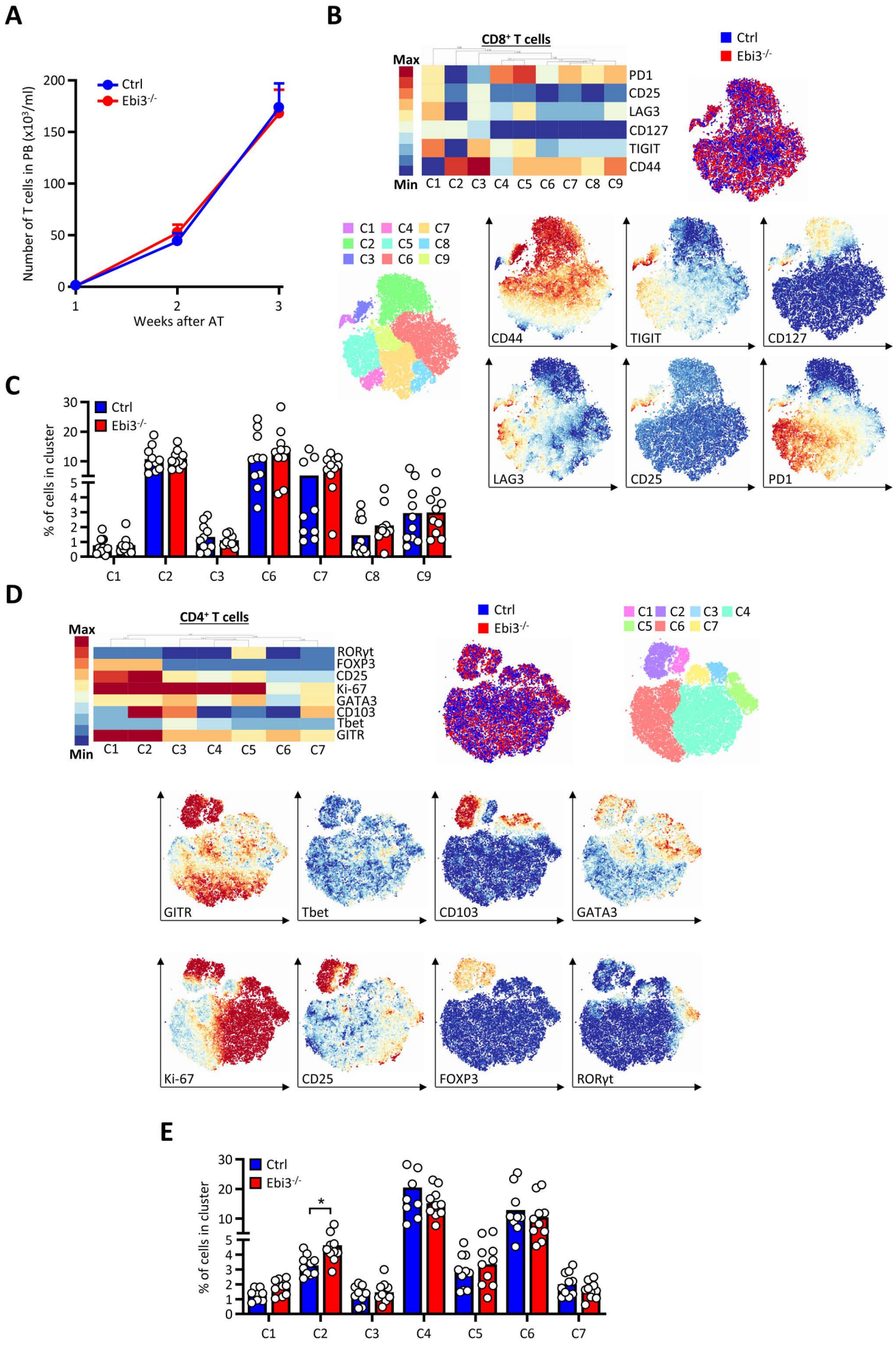
A
Number of T cells in PB (x10³/ml)
Ctrl
Ebi3-/-
Weeks after AT
B
CD8+ T cells
Max
Min
PD1
CD25
LAG3
CD127
TIGIT
CD44
C1 C2 C3 C4 C5 C6 C7 C8 C9
C
% of cells in cluster
D
CD4+ T cells
RORγt
FOXP3
CD25
Ki-67
GATA3
CD103
Tbet
GITR
E
*

Figure S5

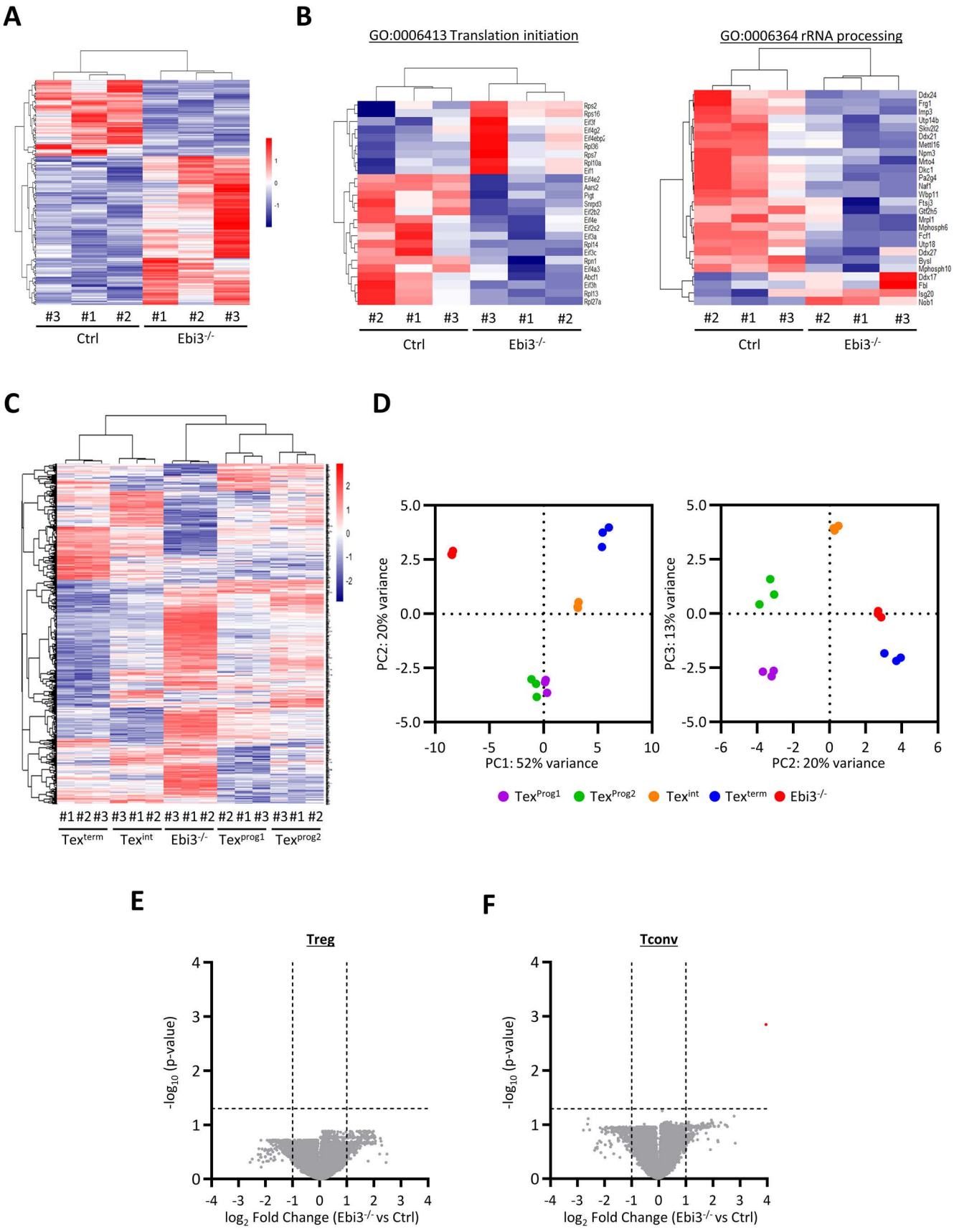
A
#3 #1 #2 #1 #2 #3
Ctrl
Ebi3-/-
B
GO:0006413 Translation initiation
Rps2
Rps16
Eif3f
Eif4g2
Eif4ebp2
Rpl36
Rps7
Rpl10a
Eif1
Eif4e2
Aars2
Pigt
Snrpd3
Eif2b2
Eif4e
Eif2s2
Eif3a
Rpl14
Eif3c
Rpn1
Eif4a3
Abcf1
Eif3h
Rpl13
Rpl27a
#2 #1 #3 #3 #1 #2
Ctrl
Ebi3-/-
GO:0006364 rRNA processing
Ddx24
Frg1
Imp3
Utp14b
Skiv2l2
Ddx21
Mettl16
Npm3
Mrto4
Dkc1
Pa2g4
Naf1
Wbp11
Ftsj3
Gtf2h5
Mrpl1
Mphosph6
Fcf1
Utp18
Ddx27
Bysl
Mphosph10
Ddx17
Fbl
Isg20
Nob1
#2 #1 #3 #2 #1 #3
Ctrl
Ebi3-/-
C
#1 #2 #3 #3 #1 #2 #3 #1 #2 #2 #1 #3 #3 #1 #2
Texterm
Texint
Ebi3-/-
Texprog1
Texprog2
D
PC2: 20% variance
PC1: 52% variance
PC3: 13% variance
PC2: 20% variance
Texprog1
Texprog2
Texint
Texterm
Ebi3-/-
E
Treg
-log10 (p-value)
log2 Fold Change (Ebi3-/- vs Ctrl)
F
Tconv
-log10 (p-value)
log2 Fold Change (Ebi3-/- vs Ctrl)

Figure S6

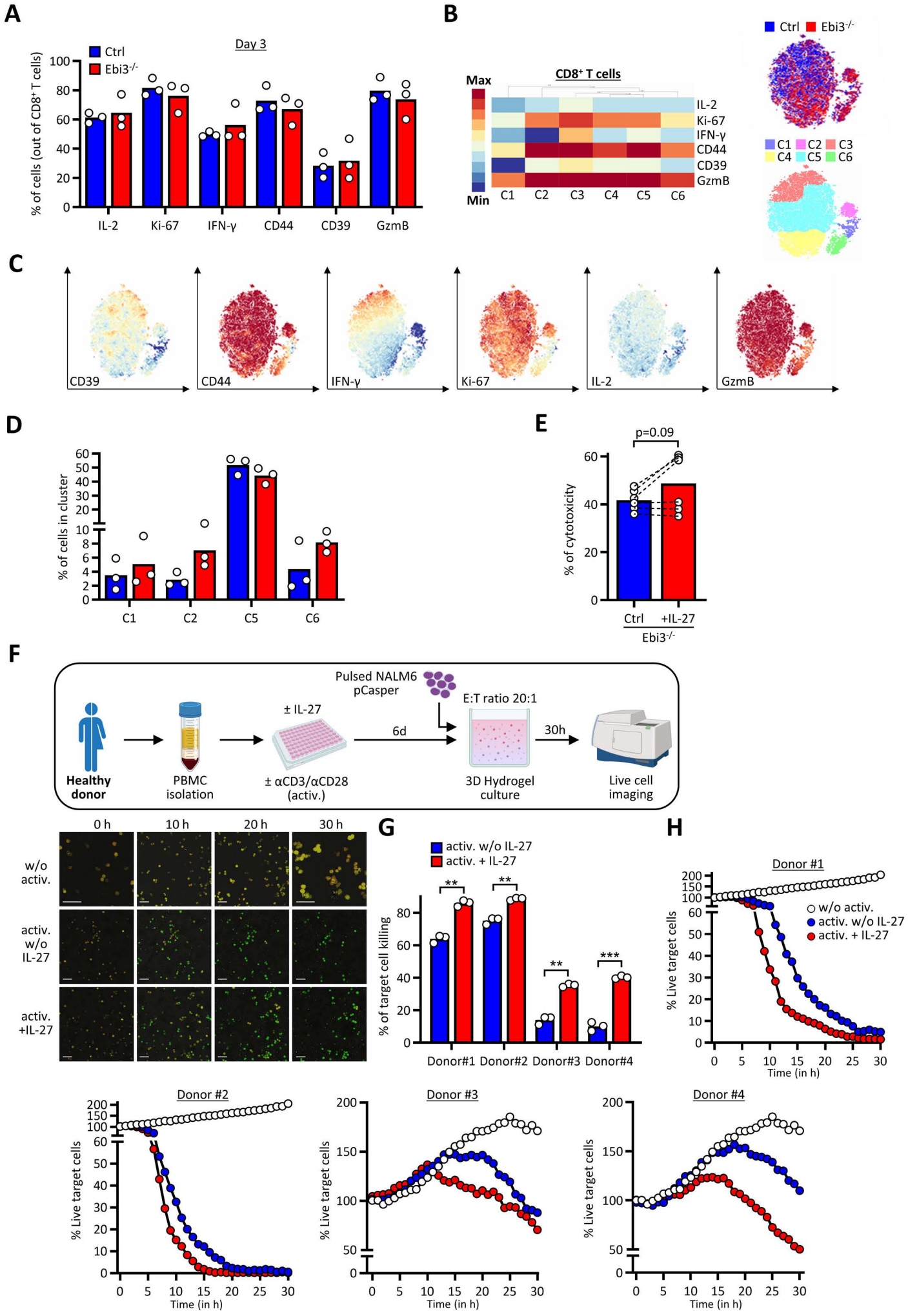
A
Day 3
Ctrl
Ebi3-/-
% of cells (out of CD8+ T cells)
IL-2
Ki-67
IFN-γ
CD44
CD39
GzmB
B
CD8+ T cells
Max
Min
C1 C2 C3 C4 C5 C6
C
CD39
CD44
IFN-γ
Ki-67
IL-2
GzmB
D
% of cells in cluster
E
p=0.09
% of cytotoxicity
Ctrl
+IL-27
Ebi3-/-
F
Healthy donor
PBMC isolation
± IL-27
± αCD3/αCD28 (activ.)
Pulsed NALM6 pCasper
6d
E:T ratio 20:1
3D Hydrogel culture
30h
Live cell imaging
0 h
10 h
20 h
30 h
w/o activ.
activ. w/o IL-27
activ. +IL-27
G
activ. w/o IL-27
activ. + IL-27
% of target cell killing
Donor#1
Donor#2
Donor#3
Donor#4
H
Donor #1
w/o activ.
activ. w/o IL-27
activ. + IL-27
% Live target cells
Time (in h)
Donor #2
Donor #3
Donor #4

Figure S7

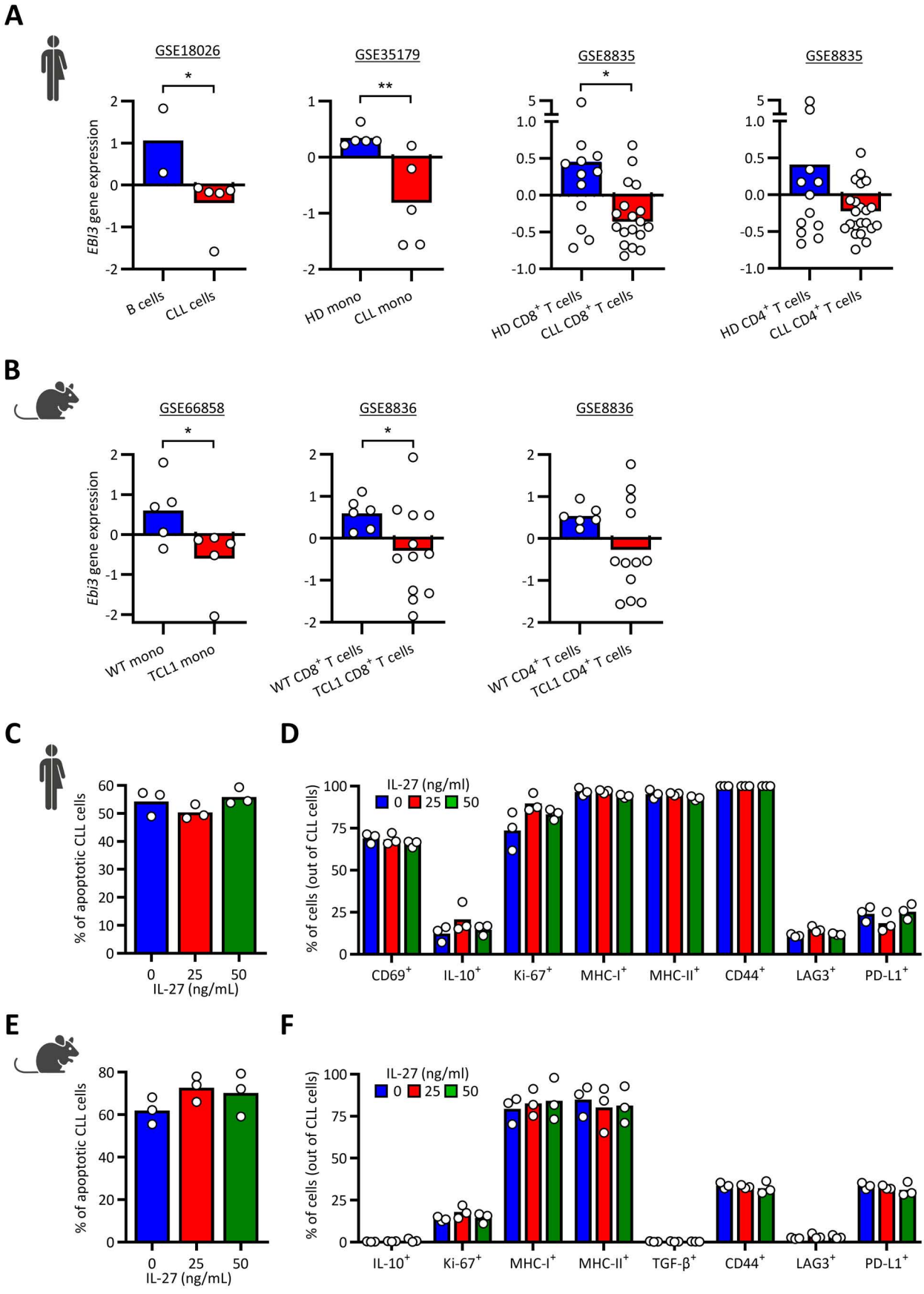
A
GSE18026
GSE35179
GSE8835
GSE8835
EBI3 gene expression
B cells
CLL cells
HD mono
CLL mono
HD CD8+ T cells
CLL CD8+ T cells
HD CD4+ T cells
CLL CD4+ T cells
B
GSE66858
GSE8836
GSE8836
Ebi3 gene expression
WT mono
TCL1 mono
WT CD8+ T cells
TCL1 CD8+ T cells
WT CD4+ T cells
TCL1 CD4+ T cells
C
% of apoptotic CLL cells
IL-27 (ng/mL)
D
IL-27 (ng/ml)
0 25 50
% of cells (out of CLL cells)
CD69+
IL-10+
Ki-67+
MHC-I+
MHC-II+
CD44+
LAG3+
PD-L1+
E
% of apoptotic CLL cells
IL-27 (ng/mL)
F
IL-27 (ng/ml)
0 25 50
% of cells (out of CLL cells)
IL-10+
Ki-67+
MHC-I+
MHC-II+
TGF-β+
CD44+
LAG3+
PD-L1+

Figure S8

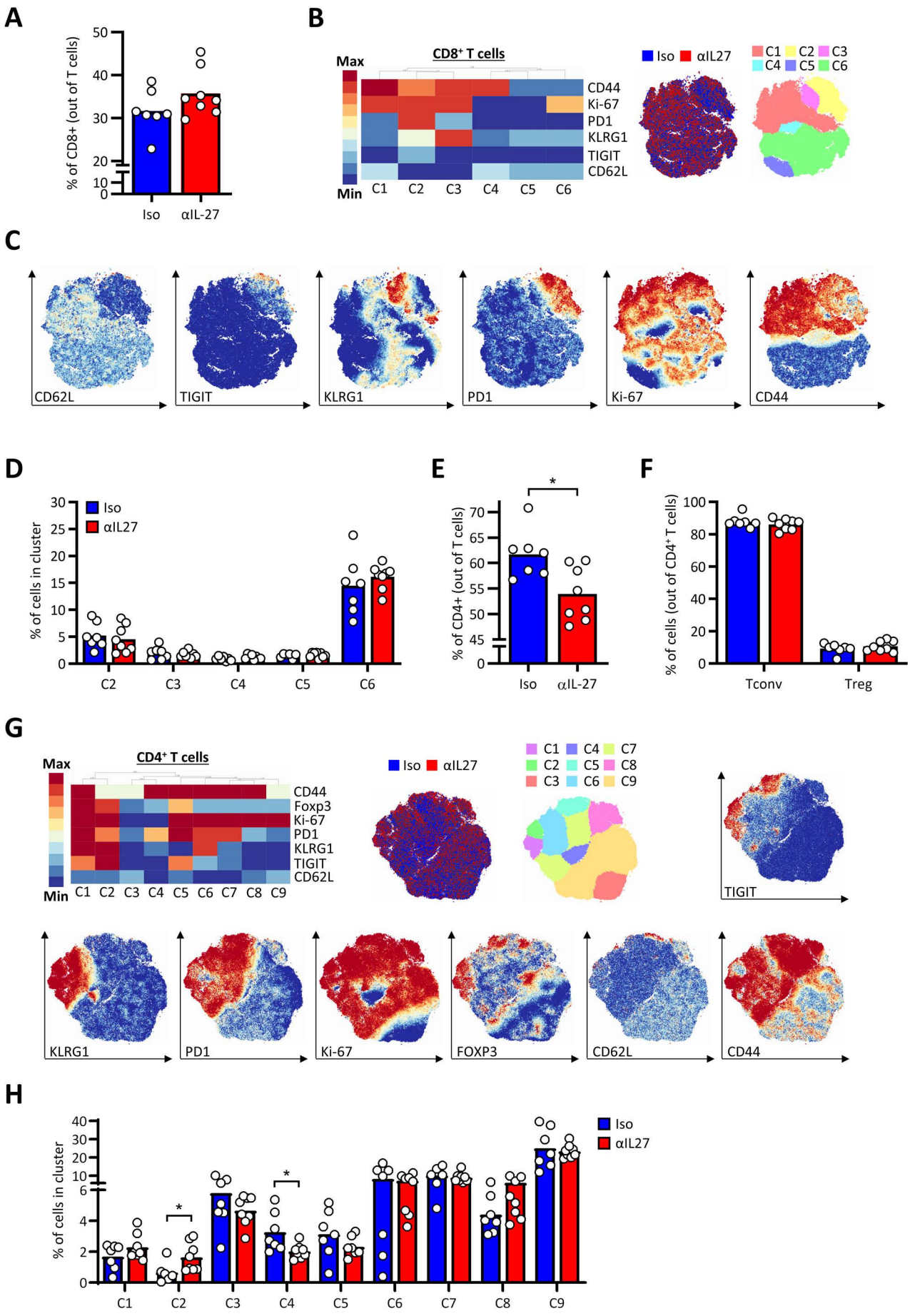
A
% of CD8+ (out of T cells)
Iso
αIL-27
B
CD8⁺ T cells
Max
Min
CD44
Ki-67
PD1
KLRG1
TIGIT
CD62L
C1 C2 C3 C4 C5 C6
Iso αIL27
C1 C2 C3 C4 C5 C6
C
CD62L
TIGIT
KLRG1
PD1
Ki-67
CD44
D
% of cells in cluster
Iso
αIL27
C2 C3 C4 C5 C6
E
% of CD4+ (out of T cells)
Iso
αIL-27
F
% of cells (out of CD4⁺ T cells)
Tconv
Treg
G
CD4⁺ T cells
Max
Min
CD44
Foxp3
Ki-67
PD1
KLRG1
TIGIT
CD62L
C1 C2 C3 C4 C5 C6 C7 C8 C9
Iso αIL27
C1 C4 C7
C2 C5 C8
C3 C6 C9
TIGIT
KLRG1
PD1
Ki-67
FOXP3
CD62L
CD44
H
% of cells in cluster
Iso
αIL27
C1 C2 C3 C4 C5 C6 C7 C8 C9